Preparation of Polymeric Nanoscale Networks from Cylindrical Molecular Bottlebrushes

Dingcai Wu,[†,*] Alper Nese,[‡,∥] Joanna Pietrasik,[§] Yeru Liang,[†] Hongkun He,[‡] Michal Kruk,[⊥] Liang Huang,[⊥,¶] Tomasz Kowalewski,[‡] and Krzysztof Matyjaszewski[‡,*]

[†]Materials Science Institute, PCFM Laboratory, School of Chemistry and Chemical Engineering, Sun Yat-sen University, Guangzhou 510275, People's Republic of China, [‡]Department of Chemistry, Carnegie Mellon University, 4400 Fifth Avenue, Pittsburgh, Pennsylvania 15213, United States, [§]Institute of Polymer and Dye Technology, Technical University of Lodz, Stefanowskiego 12/16, 90 924 Lodz, Poland, and [⊥]Center for Engineered Polymeric Materials, Department of Chemistry, College of Staten Island and Graduate Center, City University of New York, 2800 Victory Boulevard, Staten Island, New York 10314, United States. [∥]Present address: Department of Chemical Engineering and Materials Science, University of Southern California, Los Angeles, California 90089. [¶]Present address: ATRP Solutions, Pittsburgh, Pennsylvania 15213.

ABSTRACT

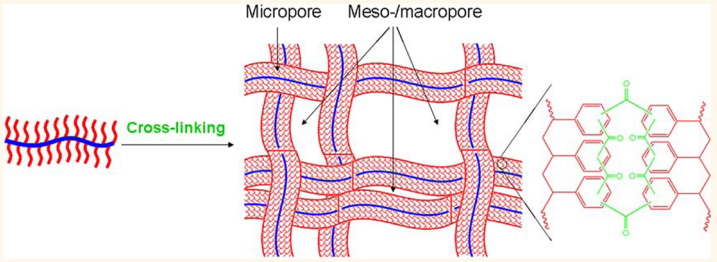

The design and control of polymeric nanoscale network structures at the molecular level remains a challenging issue. Here we construct a novel type of polymeric nanoscale networks with a unique microporous nanofiber unit employing the intra/interbrush carbonyl cross-linking of polystyrene side chains for well-defined cylindrical polystyrene molecular bottlebrushes. The size of the side chains plays a vital role in the tuning of nanostructure of networks at the molecular level. We also show that the as-prepared polymeric nanoscale networks exhibit high specific adsorption capacity per unit surface area because of the synergistic effect of their unique hierarchical porous structures. Our strategy represents a new avenue for the network unit topology and provides a new application for molecular bottlebrushes in nanotechnology.

KEYWORDS: nanoscale network · polystyrene molecular bottlebrush · cross-linking · atom transfer radical polymerization (ATRP) · nanopore · adsorption

Porous polymers, which merge the properties of both porous materials and polymers, have attracted great interest due to potential applications in adsorption, separation, catalysis, energy, sensors, biomedicine, and other areas, including precursors of nanocarbons as well as masks for nanopatterning.[1−15] Therefore, it is important to develop reliable methods for preparation of porous polymers, with designed pore architecture as well as customized polymeric framework structure.[1] In recent years, there has been a growing focus on the design and construction of three-dimensional (3D) polymeric nanoscale network structures because of their well-developed porosity and good pore interconnectivity.[9,10,16−19] These 3D nanoscale network structures should find utility in many practical applications, especially where good mass transport properties are highly desired.[9,10,16−19] While significant advances in design, fabrication, and control over topology and properties of nanoscale network structures targeting many applications have been made, accurate control over nanoscale network structures remains a challenging issue. Because the currently used nanoscale network materials are usually obtained using uncontrolled condensation or conventional free radical polymerization procedures, this leads to typical network units based on nonporous nanoparticles with ill-defined shapes and broad size distributions.[9,10,16−19] Recently, several techniques to incorporate new network units were developed by employing microporous nanoparticles and hierarchical nanospheres with a mesoporous core and microporous shell.[7,10,19] However, the prepared network units have conventional spherical shapes.

In this paper, we report the successful design and construction of a novel type of nanoscale network structure with a unique network unit (*i.e.*, microporous nanofiber), formed by utilizing cylindrical molecular brushes (bottlebrushes) with precise molecular structures as building blocks. This strategy opens the door for molecular level tailoring of the nanoscale network structures

* Address correspondence to km3b@andrew.cmu.edu, wudc@mail.sysu.edu.cn.

Received for review April 12, 2012 and accepted June 21, 2012.

Published online June 21, 2012
10.1021/nn302096d

and provides a new application for molecular brush macromolecules in nanotechnology. The novel network unit topology could provide new avenues for nanoscale network structures in other applications.

Molecular bottlebrushes form a unique class of macromolecules with linear or dendritic side chains densely grafted from a linear backbone.[20−26] Steric repulsion between the side chains forces the backbone to adopt an extended chain conformation, eventually resulting in the molecule with a cylindrical shape if the backbone is much longer than the side chains.[20−26] This paper presents the use of well-defined polystyrene (PS) molecular bottlebrush (Scheme 1) as a building block for the synthesis of materials consisting of stable cross-linked nanoscale networks. The PS side chains in the brush macromolecule were cross-linked to form an interconnected nanoscale network with a unique hierarchical porous structure by introducing carbonyl (−CO−) cross-linking bridges between the phenyl rings (Scheme 2 and Scheme S1 in Supporting Information). The cross-linking of neighboring PS chains in a molecular bottlebrush (*i.e.*, intrabrush cross-linking) forms the nanofiber network unit that contains well-developed micropores in the cross-linked framework; meanwhile, the cross-linking of PS chains on the periphery of colliding molecular bottlebrushes (*i.e.*, interbrush cross-linking) interconnects the nanofiber network units with each other in various directions, leading to formation of numerous large-sized nanopores, especially mesopores, because of the agglomeration with covalent cross-linking.

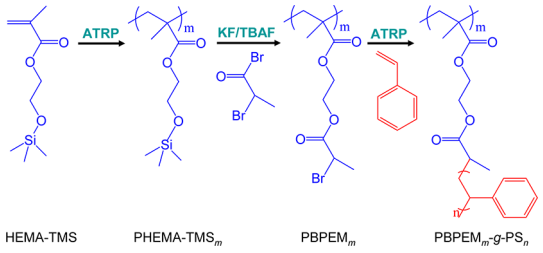

Scheme 1. Synthetic route to cylindrical polystyrene molecular brush poly(2-(2-bromopropionyloxy)ethyl methacrylate-*graft*-styrene) (PBPEM$_m$-*g*-PS$_n$).

RESULTS AND DISCUSSION

The well-defined PBPEM$_{4600}$-*g*-PS$_{200}$ with backbone DP = 4600 and side chain DP = 200 (M_w/M_n = 1.35, Figure S1A) was synthesized and then used as a representative example of PS molecular brushes. Its PS side chains underwent both intra- and interbrush cross-linking by formation of $-CCl_2-$ cross-linking bridges between the phenyl rings, which were subsequently converted into −CO− groups by hydrolysis (Scheme S1).[7,10,19,27] The formation of −CO− cross-linking bridges was confirmed by FTIR spectrum of the resulting polymeric nanoscale network NN-PBPEM$_{4600}$-*g*-PS$_{200}$ (Figure S2). Because of the introduction of the cross-linking bridges, the obtained NN-PBPEM$_{4600}$-*g*-PS$_{200}$ had a weight gain of 28%, which could be translated into the molar ratio of styrene unit to −CO− bridge approximately equal to 1, indicating a highly cross-linked structure.

This intrabrush cross-linking led to the formation of the stable unique network unit, that is, microporous nanofiber with a cross-linked structure. The nanofiber morphology was clearly observed by transmission electron microscopy (TEM) (Figure 1A,B). Theoretically, assuming a cylindrical geometry with a length $L = 0.25 \times DP_{BC}$ nm,[20] and a density $\rho = 1$ g/cm^3 $= 1 \times 10^{-21}$ g/nm^3, the nominal diameter D for PS molecular bottlebrush can be calculated as follows:

$$\rho = \frac{m}{V} = \frac{M_{n,t}/6.02 \times 10^{23}}{\pi(D/2)^2 L} = \frac{4M_{n,t}/6.02 \times 10^{23}}{\pi D^2 \times 0.25 DP_{BC}}$$

$$= \frac{16M_{n,t}/6.02 \times 10^{23}}{\pi D^2 DP_{BC}}$$

where $M_{n,t}$ is the theoretical molecular weight of the entire bottlebrush and DP_{BC} is the degree of polymerization of the backbone chain. For the PBPEM$_{4600}$-*g*-PS$_{200}$ with $M_{n,t} = 9.6 \times 10^7$ and $DP_{BC} = 4600$, the nominal diameter D is calculated as 13 nm, while the TEM image of NN-PBPEM$_{4600}$-*g*-PS$_{200}$ in Figure 1A,B gave the nanofiber diameter of about 12 nm. This indicates that the cross-linking treatment did not lead to an obvious size change of the cylindrical bottlebrush. The presence of micropores inside the nanofiber was confirmed by an adsorption uptake at low relative

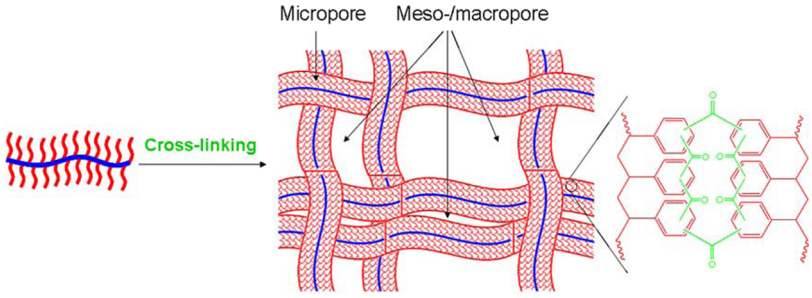

Scheme 2. Schematic illustration of the fabrication of polymeric nanoscale network based on intra-/interbrush cross-linking of soluble polystyrene bottlebrush macromolecules.

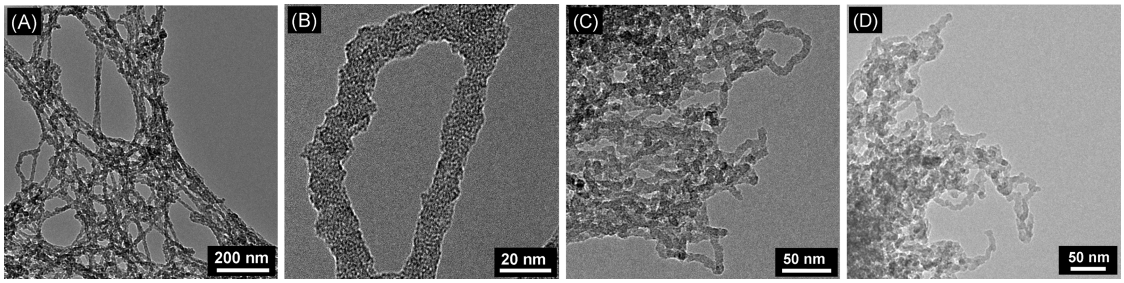

Figure 1. TEM images of nanoscale networks from polystyrene molecular brush: (A,B) NN-PBPEM$_{4600}$-*g*-PS$_{200}$; (C) NN-PBPEM$_{4600}$-*g*-PS$_{60}$; and (D) NN-PBPEM$_{400}$-*g*-PS$_{50}$.

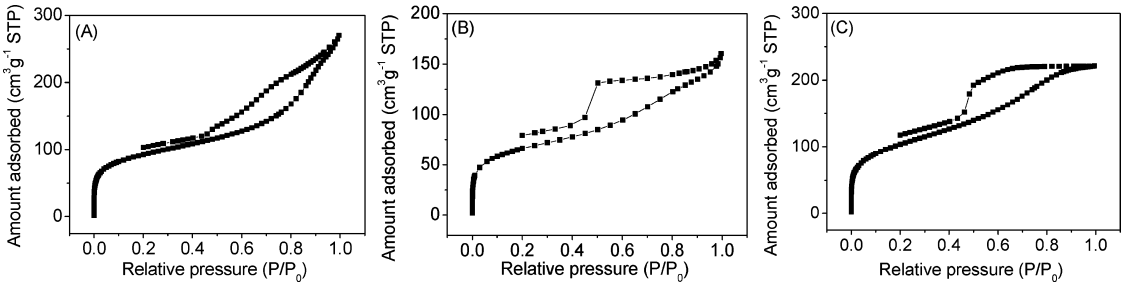

Figure 2. N_2 adsorption−desorption isotherms of (A) NN-PBPEM$_{4600}$-*g*-PS$_{200}$; (B) NN-PBPEM$_{4600}$-*g*-PS$_{60}$; and (C) NN-PBPEM$_{400}$-*g*-PS$_{50}$.

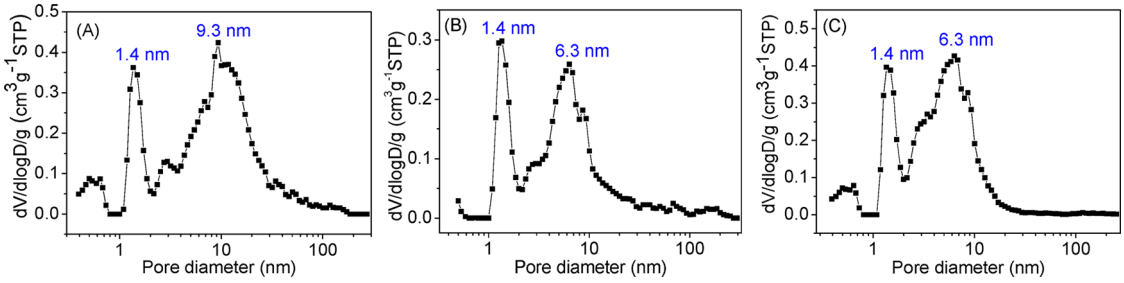

Figure 3. DFT pore size distributions of (A) NN-PBPEM$_{4600}$-*g*-PS$_{200}$; (B) NN-PBPEM$_{4600}$-*g*-PS$_{60}$; and (C) NN-PBPEM$_{400}$-*g*-PS$_{50}$.

pressure in the N_2 adsorption−desorption isotherm in Figure 2A.[28] According to the pore size distribution (PSD) curve by density functional theory (DFT)[29−33] (Figure 3A), the micropores had a maximum at about 1.4 nm.

Furthermore, during the cross-linking reaction, the PS chains on the periphery of the brushes, which had interpenetrated PS chains on nearby brush macromolecules, underwent interbrush cross-linking reactions to form a 3D polymeric nanoscale network structure, NN-PBPEM$_{4600}$-*g*-PS$_{200}$ (Figure 1A). There are three possible interbrush cross-linking modes during interbrush cross-linking reactions: end−end, end−body, and body−body cross-linking (Scheme S2). The resulting polymeric nanoscale network contains numerous mesopores and a few macropores (Figure 1A), apparently arising from close and loose aggregation of nanofiber network units (Scheme S3). Although macropores of size above ~100 nm cannot be effectively probed by nitrogen adsorption, no adsorption plateau at high relative pressure in the isotherm (Figure 2A) suggested the presence of macropores. The DFT PSD curve in Figure 3A showed that these meso-/macropores among the network had a maximum at 9.3 nm. The preferential formation of such mesopores can be ascribed to the predominant close cross-linking aggregation of nanofiber network units (Figure 1A). It should be noted that some large macropores, that is, the spaces between very loosely aggregated nanofibers, may be too large and too open to lead to capillary condensation and thus to be reflected in pore size distributions. A Brunauer−Emmett−Teller (BET) calculation gave the BET surface area for the NN-PBPEM$_{4600}$-*g*-PS$_{200}$ equal to 328 m^2 g^{-1}, and the t-plot method gave the surface areas of micropores and external large-sized pores, the majority of which is mesopore, equal to 104 and 224 m^2 g^{-1}, respectively.

In order to understand the dependence of the final nanostructure of the nanoscale networks on the initial molecular structure of PS molecular brushes, brushes with different sizes of backbone and side chains, that is, PBPEM$_{4600}$-*g*-PS$_{60}$ (M_w/M_n = 1.21, Figure S1B) and

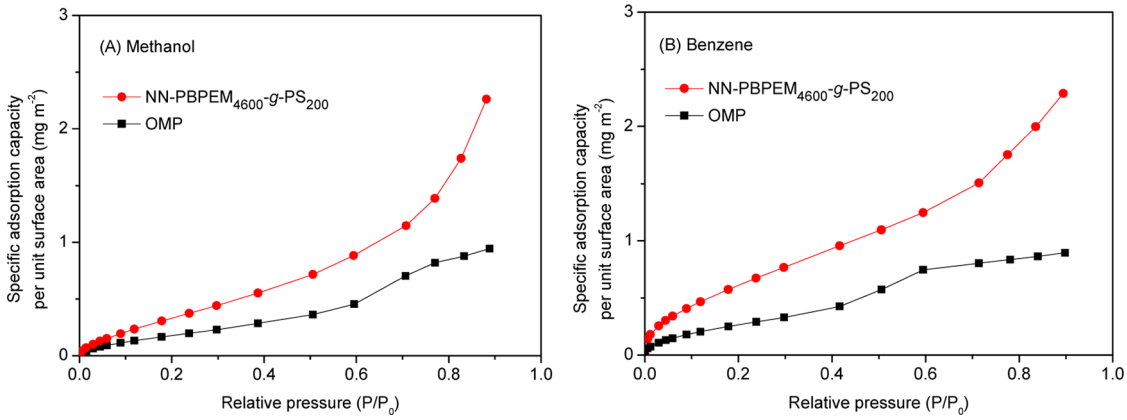

Figure 4. Specific adsorption capacity per unit surface area toward (A) methanol vapor and (B) benzene vapor at various relative pressures for NN-PBPEM$_{4600}$-*g*-PS$_{200}$ and ordered mesoporous polymer resin (OMP).

PBPEM$_{400}$-*g*-PS$_{50}$ (M_w/M_n = 1.32, Figure S1C), were synthesized and the resulting polymeric nanoscale networks NN-PBPEM$_{4600}$-*g*-PS$_{60}$ and NN-PBPEM$_{400}$-*g*-PS$_{50}$ were prepared and examined.

A comparison of the TEM images in panels A,B *versus* those in panel C in Figure 1 provides an evaluation of nanoscale networks formed from brush macromolecules with the different DPs of the side chain. As expected, a decrease in the DP of the side chains from 200 to 60 resulted in a reduction in the diameter of nanofiber network unit from ~12 to ~8 nm. Meanwhile, the maximum of PSD for interbrush network pores decreased from 9.3 to 6.3 nm (see Figure 3A *vs* 3B) because of closer cross-linking aggregation for nanofibers with smaller diameter.

Furthermore, by comparing nanoscale networks NN-PBPEM$_{4600}$-*g*-PS$_{60}$ and NN-PBPEM$_{400}$-*g*-PS$_{50}$, it can be seen that a significant decrease of the backbone DP from 4600 to 400 with similar side chain DP (60 *vs* 50) basically did not change the maximum of PSD for interbrush network pores; see Figure 3B *vs* 3C. This indicates that the mesopore size is primarily related to the diameter of the nanofibers (if the materials are prepared under the same conditions) (Figure 1), but the possibility of interbrush end−end cross-linking cannot be precluded. On the other hand, the size of micropores within network framework did not change with DPs of the backbone or side chains (Figures 2 and 3), due to the same Friedel−Crafts (F−C) reaction during the intrabrush cross-linking process.

To demonstrate usefulness and advantage of the unique hierarchical porous polymeric nanoscale networks, we studied their adsorption properties toward organic vapors and made a comparison with those of an ordered mesoporous polymer resin (OMP) with BET surface area of 472 m^2 g^{-1} and mesopore diameter of 5.0 nm (see Supporting Information) prepared by a self-assembly procedure.[34] The OMP with highly ordered 2D hexagonal mesostructure is a promising adsorbent with good mass diffusion performance. However, it is found that the NN-PBPEM$_{4600}$-*g*-PS$_{200}$ had a superior adsorption performance toward organic vapors such as methanol (Figure S3A) and benzene (Figure S3B) at various relative pressures than the OMP, although the NN-PBPEM$_{4600}$-*g*-PS$_{200}$ had a smaller BET surface area than the OMP (328 *vs* 472 m^2 g^{-1}). This indicated that the as-prepared polymeric nanoscale network had a higher specific adsorption capacity per unit surface area than the OMP. For example, for methanol adsorption (Figure 4A), the NN-PBPEM$_{4600}$-*g*-PS$_{200}$ had 0.44 and 2.26 mg m^{-2} at P/P_0 = 0.30 and 0.88, respectively, whereas the OMP had 0.23 and 0.93 mg m^{-2} at P/P_0 = 0.30 and 0.88, respectively; for benzene adsorption (Figure 4B), the NN-PBPEM$_{4600}$-*g*-PS$_{200}$ had 0.77 and 2.22 mg m^{-2} at P/P_0 = 0.30 and 0.88, respectively, whereas the OMP had 0.30 and 0.89 mg m^{-2} at P/P_0 = 0.30 and 0.88, respectively. This demonstrated that the polymeric nanoscale network has more efficient pore surface utilization, most likely due to the positive synergistic effect of their unique hierarchical micro- and meso-/macroporous structures. It should be noted that the pore surface chemistry difference between the NN-PBPEM$_{4600}$-*g*-PS$_{200}$ and the OMP could play a role, but it is secondary to the adsorption properties since the NN-PBPEM$_{4600}$-*g*-PS$_{200}$ always had a better adsorption performance toward organic vapors, whether for hydrophilic methanol or hydrophobic benzene, when compared to the OMP. In addition, the NN-PBPEM$_{4600}$-*g*-PS$_{200}$ had a higher adsorption capacity for benzene than for methanol, at low and medium P/P_0 ranges (Figure S4) because of its hydrophobic pore surfaces.

CONCLUSIONS

We have developed a new strategy for design and construction of polymeric nanoscale networks with a unique microporous nanofiber network unit based on the intra/interbrush carbonyl cross-linking of side chains of PS molecular brushes. The intrabrush cross-linking led to the formation of micropores, and the interbrush cross-linking led to the formation of large-sized nanopores (predominant mesopores) throughout

the nanoscale network. The DP of the PS side chains played an important role in the control of nanostructure of networks at the molecular level. When decreasing the side chain DP from 200 to 60, the diameter of the nanofiber network unit decreased from 12 to 8 nm, and the size of the large-sized network nanopores decreased from 9.3 to 6.3 nm. Moreover, the as-prepared polymeric nanoscale networks exhibited a higher specific adsorption capacity per unit surface area toward both methanol and benzene vapors than ordered mesoporous polymer because of the synergistic effect of their unique hierarchical porous structures. The novel polymeric nanoscale networks formed by this procedure could find some applications as adsorbents, separation media, catalyst supports, and nanomaterial templates. The new concept described here would also be useful for applying other well-defined molecular brush macromolecules to advanced nanomaterials based on cross-linking chemistry.

METHODS

Materials. All chemicals were purchased from Aldrich and used as received unless otherwise stated. Trimethylsilyl-protected 2-hydroxyethyl methacrylate (HEMA-TMS) (99%) was purchased from Scientific Polymer Products and distilled under vacuum before use. Styrene was purified by passing through a basic alumina column. CuBr was purified by washing sequentially with acetic acid and diethyl ether, filtration, and drying and was stored under nitrogen before use.

Characterization. Macromolecule samples were analyzed by a gel permeation chromatography (GPC) system conducted with a Waters 515 pump and Waters 2414 differential refractometer using PSS columns (Styrogel 10^5, 10^3, 10^2 Å) in THF as an eluent (308 K, flow rate of 1 mL/min). Linear PMMA standards were used for calibration. The hydrogen nuclear magnetic resonance (^{1}H NMR) measurements were performed on a Bruker Avance 300 MHz spectrometer at 300 K. The FTIR spectra of the polymeric nanoscale network samples were recorded on a Bruker TENSOR 27 infrared spectroscopy by a KBr disk method. The nanostructures of the polymeric nanoscale network samples were investigated by a JEM-2010HR transmission electron microscope and a Micromeritics ASAP 2020 analyzer at 77 K. The BET surface area (S_{BET}) was analyzed by Brunauer–Emmett–Teller (BET) theory. The meso-/macropore surface area (S_{ext}) was determined by t-plot method, and then the micropore surface area (S_{mic}) was obtained by subtracting the S_{ext} from the S_{BET}. The pore size distribution was obtained by performing analysis of the N_2 adsorption isotherms based on local isotherms generated using density functional theory (DFT). The DFT model assumed a carbon (graphite) surface and a slit-like pore geometry. A medium regularization was used in generating pore size distributions through the inversion of the integral equation for the adsorption isotherm. The adsorption properties toward organic vapors were studied with a Hiden IG-3 intelligent gravimetric analyzer. The specific adsorption capacity per unit surface area at various relative pressures was obtained by dividing the corresponding adsorption amount by the S_{BET}.

Synthesis. As illustrated in Scheme 1, the PS molecular brushes were synthesized by atom transfer radical polymerization (ATRP),[35−38b] one of the most widely used controlled/living radical polymerization methods, according to our previously reported procedures.[39,40] First, a macroinitiator poly(2-(2-bromopropionyloxy)ethyl methacrylate with m initiation sites (PBPEM$_m$) was synthesized by ATRP of HEMA-TMS to yield poly(HEMA-TMS) (PHEMA-TMS$_m$), followed by TMS deprotection and esterification with 2-bromopropionyl bromide. The resulting PBPEM$_m$ was used to initiate ATRP of styrene from each repeat unit by a grafting from mechanism to yield the targeted molecular brush PBPEM$_m$-g-PS$_n$. The experimental details for various PS molecular brushes were provided as follows.

Synthesis of PBPEM$_{4600}$-g-PS$_{200}$. The brushes were synthesized from poly(2-(2-bromopropionyloxy)ethyl methacrylate backbone with 4600 initiation sites (PBPEM$_{4600}$) (Figure S5A and Figure S6). A clean and dry 25 mL Schlenk flask was charged with PBPEM$_{4600}$ (0.0231 g, 0.0875 mmol), styrene (20.0 mL, 175 mmol), N,N,N',N'',N''-pentamethyldiethylenetriamine (PMDETA) (18.2 μL, 0.0875 mmol), $CuBr_2$ (2.0 mg, 0.00875 mmol), and dimethylformamide (DMF) (2.2 mL). The flask was deoxygenated by three freeze–pump–thaw cycles. During the final cycle, the flask was filled with nitrogen and CuBr (11.3 mg, 0.0788 mmol) was quickly added to the frozen mixture. The flask was sealed, evacuated, and backfilled with nitrogen five times before it was immersed in an oil bath at 50 °C for 192 h. Reaction was stopped by opening the flask to air. Polymer was purified by precipitating two times from tetrahydrofuran (THF) into methanol and drying under vacuum at room temperature overnight.

The successful incorporation of PS side chains into the as-synthesized PBPEM$_{4600}$-g-PS$_{200}$ was confirmed by ^{1}H NMR spectrum in Figure S5B. The PBPEM$_{4600}$-g-PS$_{200}$ had side chains with degree of polymerization (DP) = 200, as calculated by gravimetry,[41] assuming the essentially quantitative initiation efficiency of PBPEM macroinitiator.[42] M_n = 4 680 000 and M_w/M_n = 1.35 were determined by GPC with linear poly(methyl methacrylate) (PMMA) standards (Figure S1A). A theoretical molecular weight M_n for the brush was calculated to be M_n = 96 000 000, which was significantly larger than the apparent M_n from GPC, due to highly branched and compact bottlebrush topology.

Synthesis of PBPEM$_{4600}$-g-PS$_{60}$. A clean and dry 25 mL Schlenk flask was charged with PBPEM$_{4600}$ (0.0577 g, 0.219 mmol), styrene (20.0 mL, 175 mmol), 4,4′-di-(5-nonyl)-2,2′-bipyridine (0.179 g, 0.438 mmol), $CuBr_2$ (9.8 mg, 0.0438 mmol), and anisole (3.5 mL). The flask was deoxygenated by two freeze–pump–thaw cycles. During the final cycle, the flask was filled with nitrogen and CuBr (56.3 mg, 0.394 mmol) was quickly added to the frozen mixture. The flask was sealed, evacuated, and backfilled with nitrogen two times before it was immersed in an oil bath at 70 °C. A portion of the reaction aliquot was taken out by a syringe under nitrogen atmosphere after 157 h, giving polymer. Polymer was purified by precipitating two times from THF into methanol and drying under vacuum at room temperature overnight. Polymer had side chain DP = 60 as calculated by gravimetry. M_n = 4 360 000 and M_w/M_n = 1.21 were determined by GPC with linear PMMA standards (Figure S1B).

Synthesis of PBPEM$_{400}$-g-PS$_{50}$. Synthesis of PBPEM$_{400}$ (the brush backbone with 400 initiation sites) was performed by following a previously reported procedure.[40] Polymer was characterized by using GPC with linear PMMA standards giving M_n = 83 600 and M_w/M_n = 1.18. A clean and dry 25 mL Schlenk flask was charged with PBPEM$_{400}$ (0.095 g, 0.36 mmol), styrene (16.5 mL, 144 mmol), 4,4′-di-(5-nonyl)-2,2′-bipyridine (0.589 g, 1.44 mmol), $CuBr_2$ (8.0 mg, 0.036 mmol), and anisole (1.0 mL). The flask was deoxygenated by two freeze–pump–thaw cycles. During the final cycle, the flask was filled with nitrogen and CuBr (97.8 mg, 0.684 mmol) was quickly added to the frozen mixture. The flask was sealed, evacuated, and backfilled with nitrogen four times before it was immersed in an oil bath at 70 °C for 23 h. Reaction was stopped by opening the flask to air. Polymer was purified by precipitating two times from THF into methanol and drying under vacuum at room temperature overnight. Polymer had side chain DP = 50 as calculated by gravimetry. M_n = 574 000 and M_w/M_n = 1.32 were determined by GPC with linear PMMA standards (Figure S1C).

Preparation of Polymeric Nanoscale Networks. To achieve the targeted 3D nanoscale network structure, the PS side chains in the PBPEM$_{4600}$-*g*-PS$_{200}$ brush macromolecule were cross-linked in a F−C reaction in which carbon tetrachloride (CCl_4) was a solvent and also a cross-linker and anhydrous aluminum chloride ($AlCl_3$) was a F−C catalyst.[7,10,19] First, 5.00 g of $AlCl_3$ and 50 mL of CCl_4 were mixed and then heated at 75 °C for 0.5 h with magnetic stirring in a three-neck flask with a condenser. Then, 0.50 g of PBPEM$_{4600}$-*g*-PS$_{200}$ was dissolved into 50 mL of CCl_4 and was subsequently transferred to the above mixture, followed by heating at 75 °C for 24 h with magnetic stirring. One hundred milliliters of 1 M HCl was added slowly to the above mixture and then was heated at 75 °C for 1 h with magnetic stirring. The resulting yellow-brown precipitate was filtered off, washed with acetone, 1 M HCl, and pure water, followed by vacuum drying at room temperature overnight, giving the polymeric nanoscale network NN-PBPEM$_{4600}$-*g*-PS$_{200}$. NN-PBPEM$_{4600}$-*g*-PS$_{60}$ and NN-PBPEM$_{400}$-*g*-PS$_{50}$ were prepared according to the above procedure.

Conflict of Interest: The authors declare no competing financial interest.

Acknowledgment. We acknowledge financial support from National Science Foundation (DMR 09-69301 and CTS 03-04568), NSFC (51173213 and 50802116), the Fundamental Research Funds for the Central Universities (09lgpy18) and SRFDP (200805581014). We thank Wojciech Chaladaj and Janusz Jurczak for their help in synthesizing macroinitiators, and Chin Ming Hui for his help in N_2 adsorption measurement.

Supporting Information Available: Experimental details of PBPEM$_{4600}$ and OMP, formation mechanism of −CO− cross-linking bridge, cross-linking modes, cross-linking aggregation, ^{1}H NMR spectra, GPC traces, FTIR spectra, adsorption isotherms of organic vapors, and comparison of adsorption capacities. This material is available free of charge *via* the Internet at http://pubs.acs.org.

REFERENCES AND NOTES

1. Wu, D.; Xu, F.; Sun, B.; Fu, R.; He, H.; Matyjaszewski, K. Design and Preparation of Porous Polymers. *Chem. Rev.* **2012**, 10.1021/cr200440z.
2. Pitet, L. M.; Amendt, M. A.; Hillmyer, M. A. Nanoporous Linear Polyethylene from a Block Polymer Precursor. *J. Am. Chem. Soc.* **2010**, *132*, 8230–8231.
3. Jackson, E. A.; Hillmyer, M. A. Nanoporous Membranes Derived from Block Copolymers: From Drug Delivery to Water Filtration. *ACS Nano* **2010**, *4*, 3548–3553.
4. Hillmyer, M. A. Nanoporous Materials from Block Copolymer Precursors. *Adv. Polym. Sci.* **2005**, *190*, 137–181.
5. Cohen, N.; Silverstein, M. S. Synthesis of Emulsion-Templated Porous Polyacrylonitrile and Its Pyrolysis to Porous Carbon Monoliths. *Polymer* **2011**, *52*, 282–287.
6. Lumelsky, Y.; Silverstein, M. S. Biodegradable Porous Polymers through Emulsion Templating. *Macromolecules* **2009**, *42*, 1627–1633.
7. Wu, D.; Hui, C. M.; Dong, H.; Pietrasik, J.; Ryu, H. J.; Li, Z.; Zhong, M.; He, H.; Kim, E. K.; Jaroniec, M.; *et al.* Nanoporous Polystyrene and Carbon Materials with Core−Shell Nanosphere-Interconnected Network Structure. *Macromolecules* **2011**, *44*, 5846–5849.
8. Su, D. S.; Schlögl, R. Nanostructured Carbon and Carbon Nanocomposites for Electrochemical Energy Storage Applications. *ChemSusChem* **2010**, *3*, 136–168.
9. Dresselhaus, M. S. Future Directions in Carbon Science. *Annu. Rev. Mater. Sci.* **1997**, *27*, 1–34.
10. Zou, C.; Wu, D.; Li, M.; Zeng, Q.; Xu, F.; Huang, Z.; Fu, R. Template-Free Fabrication of Hierarchical Porous Carbon by Constructing Carbonyl Crosslinking Bridges between Polystyrene Chains. *J. Mater. Chem.* **2010**, *20*, 731–735.
11. Schacher, F.; Ulbricht, M.; Müller, A. H. E. Self-Supporting, Double Stimuli-Responsive Porous Membranes from Polystyrene-*Block*-Poly(*N*,*N*-dimethylaminoethyl methacrylate) Diblock Copolymers. *Adv. Funct. Mater.* **2009**, *19*, 1040–1045.
12. Abidian, M. R.; Kim, D. H.; Martin, D. C. Conducting-Polymer Nanotubes for Controlled Drug Release. *Adv. Mater.* **2006**, *18*, 405–409.
13. Pulko, I.; Wall, J.; Krajnc, P.; Cameron, N. R. Ultra-High Surface Area Functional Porous Polymers by Emulsion Templating and Hypercrosslinking: Efficient Nucleophilic Catalyst Supports. *Chem.—Eur. J.* **2010**, *16*, 2350–2354.
14. Park, S.; Wang, J.-Y.; Kim, B.; Russell, T. P. From Nanorings to Nanodots by Patterning with Block Copolymers. *Nano Lett.* **2008**, *8*, 1667–1672.
15. Zhou, N.; Bates, F. S.; Lodge, T. P. Mesoporous Membrane Templated by a Polymeric Bicontinuous Microemulsion. *Nano Lett.* **2006**, *6*, 2354–2357.
16. Al-Muhtaseb, S. A.; Ritter, J. A. Preparation and Properties of Resorcinol-Formaldehyde Organic and Carbon Gels. *Adv. Mater.* **2003**, *15*, 101–114.
17. Wu, D.; Fu, R.; Dresselhaus, M. S.; Dresselhaus, G. Fabrication and Nano-Structure Control of Carbon Aerogels *via* a Microemulsion-Templated Sol−Gel Polymerization Method. *Carbon* **2006**, *44*, 675–681.
18. Wu, D.; Fu, R.; Zhang, S.; Dresselhaus, M. S.; Dresselhaus, G. Preparation of Low-Density Carbon Aerogels by Ambient Pressure Drying. *Carbon* **2004**, *42*, 2033–2039.
19. Zeng, Q.; Wu, D.; Zou, C.; Xu, F.; Fu, R.; Li, Z.; Liang, Y.; Su, D. Template-Free Fabrication of Hierarchical Porous Carbon Based on Intra-/Inter-Sphere Crosslinking of Monodisperse Styrene-Divinylbenzene Copolymer Nanospheres. *Chem. Commun.* **2010**, *46*, 5927–5929.
20. Sheiko, S. S.; Sumerlin, B. S.; Matyjaszewski, K. Cylindrical Molecular Brushes: Synthesis, Characterization, and Properties. *Prog. Polym. Sci.* **2008**, *33*, 759–785.
21. Lee, H.-i.; Pietrasik, J.; Sheiko, S. S.; Matyjaszewski, K. Stimuli-Responsive Molecular Brushes. *Prog. Polym. Sci.* **2010**, *35*, 24–44.
22. Yuan, J.; Xu, Y.; Walther, A.; Bolisetty, S.; Schumacher, M.; Schmalz, H.; Ballauff, M.; Müller, A. H. E. Water-Soluble Organo-Silica Hybrid Nanowires. *Nat. Mater.* **2008**, *7*, 718–722.
23. Huang, K.; Rzayev, J. Well-Defined Organic Nanotubes from Multicomponent Bottlebrush Copolymers. *J. Am. Chem. Soc.* **2009**, *131*, 6880–6885.
24. Bolton, J.; Bailey, T. S.; Rzayev, J. Large Pore Size Nanoporous Materials from the Self-Assembly of Asymmetric Bottlebrush Block Copolymers. *Nano Lett.* **2011**, *11*, 998–1001.
25. Zhao, L.; Byun, M.; Rzayev, J.; Lin, Z. Polystyrene-Polylactide Bottlebrush Block Copolymer at the Air/Water Interface. *Macromolecules* **2009**, *42*, 9027–9033.
26. Zhang, M.; Breiner, T.; Moria, H.; Müller, A. H. E. Amphiphilic Cylindrical Brushes with Poly(acrylic acid) Core and Poly(*N*-butyl acrylate) Shell and Narrow Length Distribution. *Polymer* **2003**, *44*, 1449–1458.
27. Hradil, J.; Králová, E. Styrene-Divinylbenzene Copolymers Post-Crosslinked with Tetrachloromethane. *Polymer* **1998**, *39*, 6041–6048.
28. Gregg, S. J.; Sing, K. S. W. *Adsorption, Surface Area and Porosity*; Academic Press: New York, 1982; p 195.
29. Jagiello, J.; Olivier, J. P. A Simple Two-Dimensional NLDFT Model of Gas Adsorption in Finite Carbon Pores. Application to Pore Structure Analysis. *J. Phys. Chem. C* **2009**, *113*, 19382–19385.
30. Lastoskie, C.; Gubbins, K. E.; Quirke, N. Pore Size Heterogeneity and the Carbon Slit Pore: A Density Functional Theory Model. *Langmuir* **1993**, *9*, 2693–2702.
31. Ravikovitch, P. I.; Vishnyakov, A.; Russo, R.; Neimark, A. V. Unified Approach to Pore Size Characterization of Microporous Carbonaceous Materials from N_2, Ar, and CO_2 Adsorption Isotherms. *Langmuir* **2000**, *16*, 2311–2320.
32. Jagiello, J.; Thommes, M. Comparison of DFT Characterization Methods Based on N_2, Ar, CO_2, and H_2 Adsorption Applied to Carbons with Various Pore Size Distributions. *Carbon* **2004**, *42*, 1227–1232.
33. Neimark, A. V.; Ravikovitch, P. I.; Grün, M.; Schüth, F.; Unger, K. K. Pore Size Analysis of MCM-41 Type Adsorbents by Means of Nitrogen and Argon Adsorption. *J. Colloid Interface Sci.* **1998**, *207*, 159–169.

34. Zhang, F.; Meng, Y.; Gu, D.; Yan, Y.; Chen, Z.; Tu, B.; Zhao, D. An Aqueous Cooperative Assembly Route to Synthesize Ordered Mesoporous Carbons with Controlled Structures and Morphology. *Chem. Mater.* **2006**, *18*, 5279–5288.
35. Matyjaszewski, K.; Xia, J. Atom Transfer Radical Polymerization. *Chem. Rev.* **2001**, *101*, 2921–2990.
36. Wang, J.-S.; Matyjaszewski, K. Controlled/″Living″ Radical Polymerization. Atom Transfer Radical Polymerization in the Presence of Transition-Metal Complexes. *J. Am. Chem. Soc.* **1995**, *117*, 5614–5615.
37. Tsarevsky, N. V.; Matyjaszewski, K. ″Green″ Atom Transfer Radical Polymerization: From Process Design to Preparation of Well-Defined Environmentally Friendly Polymeric Materials. *Chem. Rev.* **2007**, *107*, 2270–2299.
38. (a) Matyjaszewski, K.; Tsarevsky, N. V. Nanostructured Functional Materials Prepared by Atom Transfer Radical Polymerization. *Nat. Chem.* **2009**, *1*, 276–288. (b) Matyjaszewski, K. Atom Transfer Radical Polymerization (ATRP): Current Status and Future Perspectives. *Macromolecules* **2012**, *45*, 4015–4039. (c) Matyjaszewski, K.; Spanswick, J. Copper-Mediated Atom Transfer Radical Polymerization. In *Polymer Science: A Comprehensive Reference*; Matyjaszewski, K., Möller, M., Eds; Elsevier BV: Amsterdam, 2012; Vol. 3, pp 377−428.
39. Kwiatkowski, P.; Jurczak, J.; Pietrasik, J.; Jakubowski, W.; Mueller, L.; Matyjaszewski, K. High Molecular Weight Polymethacrylates by AGET ATRP under High Pressure. *Macromolecules* **2008**, *41*, 1067–1069.
40. Beers, K. L.; Gaynor, S. G.; Matyjaszewski, K. The Synthesis of Densely Grafted Copolymers by Atom Transfer Radical Polymerization. *Macromolecules* **1998**, *31*, 9413–9415.
41. Nese, A.; Sheiko, S. S.; Matyjaszewski, K. Effect of Residual Copper on Stability of Molecular Brushes Prepared by Atom Transfer Radical Polymerization. *Eur. Polym. J.* **2011**, *47*, 1198–1202.
42. Sumerlin, B. S.; Neugebauer, D.; Matyjaszewski, K. Initiation Efficiency in the Synthesis of Molecular Brushes by Grafting from *via* Atom Transfer Radical Polymerization. *Macromolecules* **2005**, *38*, 702–708.